

Enhancing Pre-Trained Model-Based Class-Incremental Learning through Neural Collapse

Kun He^{*1} Zijian Song^{*1} Shuoxi Zhang¹ John E. Hopcroft²

¹ Huazhong University of Science and Technology ² Cornell University

Abstract

Class-Incremental Learning (CIL) is a critical capability for real-world applications, enabling learning systems to adapt to new tasks while retaining knowledge from previous ones. Recent advancements in pre-trained models (PTMs) have significantly advanced the field of CIL, demonstrating superior performance over traditional methods. However, understanding how features evolve and are distributed across incremental tasks remains an open challenge. In this paper, we propose a novel approach to modeling feature evolution in PTM-based CIL through the lens of neural collapse (NC), a striking phenomenon observed in the final phase of training, which leads to a well-separated, equiangular feature space. We explore the connection between NC and CIL effectiveness, showing that aligning feature distributions with the NC geometry enhances the ability to capture the dynamic behavior of continual learning. Based on this insight, we introduce Neural Collapse-inspired Pre-Trained Model-based CIL (NCPTM-CIL), a method that dynamically adjusts the feature space to conform to the elegant NC structure, thereby enhancing the continual learning process. Extensive experiments demonstrate that NCPTM-CIL outperforms state-of-the-art methods across four benchmark datasets. Notably, when initialized with ViT-B/16-IN1K, NCPTM-CIL surpasses the runner-up method by 6.73% on VTAB, 1.25% on CIFAR-100, and 2.5% on OmniBenchmark.

1. Introduction

In recent decades, deep learning has made remarkable strides in the field of computer vision, leading to significant advancements in performance across various downstream tasks, including image classification [7, 15, 16, 21], object recognition [4, 12, 32], and semantic segmentation [6, 68, 69], among others. However, most existing models are designed to operate in an offline training setup, limiting their ability to adapt once deployed. In real-world

scenarios, data arrives in a continuous stream, with new categories constantly emerging. Consequently, deployed models are prone to performance degradation and obsolescence, as they fail to accommodate the evolving data distribution.

To mitigate the resource burden associated of constant retraining, a widely adopted approach is Class-Incremental Learning (CIL), which allows models to incrementally update their knowledge with data from new categories. However, CIL is often plagued by the challenge of *catastrophic forgetting*, wherein the acquisition of new knowledge leads to a significant decline in performance on previously learned tasks.

Conventionally, CIL methods train models FROM SCRATCH with randomly initialized weights. However, with the rise of PRE-TRAINED MODELS (PTMs) [7], combining PTMs with CIL has emerged as a promising solution. PTMs, with their powerful generalization capabilities, have shown substantial improvements over methods trained from scratch, making them a valuable asset for CIL.

Inspired by the efficient tuning of large language models [29], recent PTM-based CIL methods have adopted prompt-based mechanisms [44, 55, 56]. These methods freeze the pre-trained backbone and append a small set of additional tokens (*i.e.*, prompts) to the input, which are optimized to adapt to incremental tasks, typically by selecting and refining task-specific prompts from a prompt pool to improve model adaptability. While these approaches show promise, the underlying mechanism of prompt optimization remains inadequately understood, and the overlap of prompts between tasks can lead to conflicts, causing catastrophic forgetting.

Another line of research, feature-based PTM-CIL [35, 65, 70, 72], leverages the strong semantic representations of PTMs to guide continual learning. These approaches assume that PTMs capture rich feature representations, enabling effective generalization to continual learning tasks. Typically, they often rely on prototype-based classification, where each instance is assigned to the class whose centroid is most similar. However, due to the inherent feature drift in continual learning, it remains unclear whether this naïve paradigm results in an optimal classifier space. Fur-

^{*}Equal contribution to this work.

thermore, the question of *how feature distributions evolve across tasks in continual learning scenarios* has not been adequately explored. We argue that understanding these dynamics is essential for fully leveraging the semantic power of pre-trained models in CIL.

In this paper, we investigate how feature distributions should evolve in PTM-based CIL. Specifically, we model this evolution using neural collapse (NC) [38]. NC describes a geometric structure that emerges in the final phase of training, where features collapse to their respective class prototypes, resulting in a well-separated, simplex equiangular tight frame (ETF). We begin with an empirical analysis of the relationship between NC and the effectiveness of CIL methods. Observing the benefits of NC for continual learning, we propose Neural Collapse-inspired Pre-trained Model-based Class-Incremental Learning (NCPTM-CIL). In this approach, we leverage the semantic features of pre-trained models to fit an ETF-based NC structure. Rather than using a fixed ETF classifier, we design a DYNAMIC ETF CLASSIFIER that can incorporate new classes and adjust to preserve the NC structure. This adjustment is achieved through an ETF ALIGNMENT. Additionally, we introduce a PULL-AND-PUSH LOSS, which drives features toward their classifier prototypes while maximizing class separation, thus improving the decision boundary.

In our extensive experimental evaluation, NCPTM-CIL achieves state-of-the-art performance on most datasets. Notably, when initialized with ViT-B/16-IN1K, NCPTM-CIL surpasses the runner-up method by 6.73% on VTAB, 1.25% on CIFAR-100, and 2.5% on OmniBenchmark. Furthermore, when compared to the upper bound of joint learning, NCPTM-CIL achieves results that are within 1.5% (CIFAR-100) and 0.52% (OmniBenchmark) of the upper bound, showcasing its potential to approach the theoretical limit of continual learning.

Our main contributions can be summarized as follows:

- We model feature evolution in PTM-based CIL using the NC structure, providing a new perspective on the dynamics of continual learning.
- We introduce a dynamic ETF classifier, ETF alignment, and PAP loss, which together constitute the core contributions of our method, enabling the dynamic maintenance of the NC structure in continual learning tasks.
- Our experimental results highlight the superiority of NCPTM-CIL and underscore the potential of neural collapse as a promising framework for advancing continual learning.

2. Related Work

2.1. Class-Incremental Learning

Class-incremental learning requires a model to continuously acquire new class semantics while retaining knowl-

edge from previous tasks. One group of approaches [42, 43, 51, 60] involves progressively expanding the network architecture, with a dedicated parameter subspace allocated for each new task to mitigate forgetting of prior knowledge. Another line of research [2, 40, 49, 50, 52] focuses on storing raw data from previous tasks, which can be combined with new data during the training of subsequent tasks to mitigate hyperplane deviation from the original feature space. Regularization-based approaches primarily propose applying penalty terms to regularize training parameters [3, 26, 28, 63] or to distill knowledge [18] from the old task model [8, 19, 25, 31, 33, 41, 58, 66].

2.2. Pre-trained Model-based Class-Incremental Learning

Pre-trained models generally exhibit powerful semantic representation capabilities. Consequently, with the increasing prominence of pre-trained models, their integration with incremental learning has become a key research focus within the field of class-incremental learning (CIL) [35, 53, 71]. In general, approaches for leveraging pre-trained models in incremental learning tasks fall into two main categories. The first category [44, 55, 56] optimizes prompts during training, which are added to the input to encode task-specific information, thereby preserving old knowledge. The second research line focuses on utilizing the robust semantic representations of pre-trained models to improve performance in continual learning. For example, Aper [70] leverages the semantic information from pre-trained features and accumulates class means as classifier. Similarly, [35] employs an online LDA classifier to reduce class-wise correlations, thereby improving separability. Moreover, [72] allocates task-specific subspaces to each task.

2.3. Neural Collapse

Neural Collapse (NC) describes an elegant mathematical structure that emerges in the terminal phase of deep model training, in which the features of the last layer and the classifier converge to form a simplex equiangular tight frame [38]. Numerous studies have consistently demonstrated the pervasive occurrence of NC across different settings, including models trained with cross-entropy [9, 13, 23, 34, 57, 75], mean squared error (MSE) [14, 36, 39, 46, 73], and even within contrastive learning [54] frameworks. Recent studies have attempted to induce NC in various domains, including imbalanced learning [1, 45, 59, 61], semantic segmentation [69], transfer learning [10, 30], and federated learning [22].

Definition 1 (Simplex ETF). *A simplex equiangular tight frame consists of a set of vectors $\mathbf{m}_i \in \mathbb{R}^d$, where $i = 1, 2, \dots, K$, with $d \geq K - 1$, satisfying the following con-*

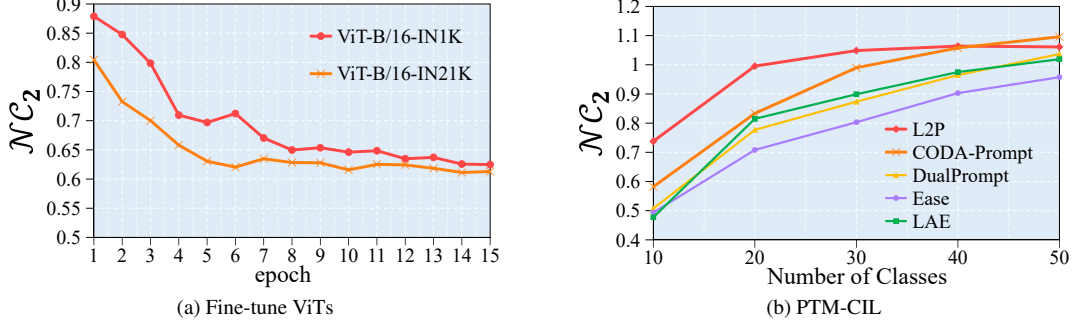


Figure 1. (a): The \mathcal{NC}_2 metric with respect to the number of epochs during fine-tuning for ViT-B/16-IN1K and ViT-B/16-IN21K. (b): The \mathcal{NC}_2 values of different PTM-CIL methods on the VTAB dataset during the incremental learning phase, where VTAB is divided into five incremental learning tasks, each containing 10 classes.

dition:

$$\mathbf{M} = \sqrt{\frac{K}{K-1}} \mathbf{U} \left(\mathbf{I}_K - \frac{1}{K} \mathbf{1}_K \mathbf{1}_K^T \right), \quad (1)$$

where $\mathbf{I}_K \in \mathbb{R}^{K \times K}$ is the identity matrix, $\mathbf{1}_K \in \mathbb{R}^K$ is a vector of all ones, and $\mathbf{U} \in \mathbb{R}^{d \times K}$ is a partial orthogonal matrix, satisfying $\mathbf{U}^T \mathbf{U} = \mathbf{I}_K$.

For simplicity, let the last-layer feature $\mathbf{f}(\mathbf{x}_i^k)$ of the sample \mathbf{x}_i^k (the i -th sample from the k -th class) be denoted as \mathbf{h}_i^k . The k -th CLASS MEANS and GLOBAL MEAN of the features are calculated as follows:

$$\mathbf{h}^k := \frac{1}{N} \sum_{i=1}^N \mathbf{h}_i^k, \quad \mathbf{h}^G := \frac{1}{K} \sum_{k=1}^K \mathbf{h}^k.$$

It is assumed that each class contains N samples, and K denotes the number of classes. Neural collapse can be quantified using the following metrics[38]:

1. **NC1: Within-class variability collapse.** \mathcal{NC}_1 describes the relative magnitude of within-class variability, defined as $\Sigma_{\mathbf{W}} = \frac{1}{NK} \sum_{k=1}^K \sum_{n=1}^N (\mathbf{h}_i^k - \mathbf{h}^k)(\mathbf{h}_i^k - \mathbf{h}^k)^\top$, in relation to the total variability. To compute \mathcal{NC}_1 , we use the within-class covariance $\Sigma_{\mathbf{W}}$ and the between-class covariance $\Sigma_{\mathbf{B}} = \frac{1}{K} \sum_{k=1}^K (\mathbf{h}^k - \mathbf{h}^G)(\mathbf{h}^k - \mathbf{h}^G)^\top$. The collapse of \mathcal{NC}_1 can be quantified by comparing the magnitude of the between-class covariance $\Sigma_{\mathbf{B}} \in \mathbb{R}^{d \times d}$ to the within-class covariance $\Sigma_{\mathbf{W}} \in \mathbb{R}^{d \times d}$ of the learned features using the following relationship:

$$\mathcal{NC}_1 := \frac{1}{K} \text{Trace} \left(\Sigma_{\mathbf{W}} \Sigma_{\mathbf{B}}^\dagger \right), \quad (2)$$

where $\Sigma_{\mathbf{B}}^\dagger$ is the pseudoinverse of $\Sigma_{\mathbf{B}}$, and Trace is the sum of the diagonal elements of a matrix.

2. **NC2: Convergence of the class mean matrix H to Simplex ETF.** For the class mean matrix $H = [\mathbf{h}^1 -$

$\mathbf{h}^G, \dots, \mathbf{h}^K - \mathbf{h}^G]$, we measure its proximity to the Simplex ETF through:

$$\mathcal{NC}_2 = \left\| \frac{HH^\top}{\|HH^\top\|_F} - \frac{1}{\sqrt{K-1}} \left(\mathbf{I}_K - \frac{1}{K} \mathbf{1}_K \mathbf{1}_K^T \right) \right\|_F. \quad (3)$$

where $\|\cdot\|_F$ is the Frobenius norm.

3. **NC3: Convergence to self-duality.** The within-class means centered by the global mean will align with their corresponding classifier weights, which implies that the classifier weights W will converge to the same simplex ETF:

$$\mathcal{NC}_3 = \left\| \frac{HW}{\|HW\|_F} - \frac{1}{\sqrt{K-1}} \left(\mathbf{I}_K - \frac{1}{K} \mathbf{1}_K \mathbf{1}_K^T \right) \right\|_F. \quad (4)$$

3. Preliminaries

3.1. Class-Incremental Learning Setup

In the scenario of class-incremental learning, a deep model $\Phi(\mathbf{f}(\cdot))$, composed of a classifier $\Phi(\cdot)$ and a backbone $\mathbf{f}(\cdot)$, aims to sequentially learn to classify an expanding set of classes so that the model can classify test samples from any task. Specifically, at each incremental step t , the model is presented with a unique set of classes \mathcal{C}_t and corresponding data $\mathcal{D}_t = \{(\mathbf{x}_i, y_i) \mid y_i \in \mathcal{C}_t\}$, where $\mathcal{C}_t \cap \mathcal{C}_{t'} = \emptyset$ for any $t \neq t'$. The task is for $\Phi(\mathbf{f}(\cdot))$ to learn each \mathcal{C}_t in sequence without revisiting the previous data. The performance of the model at the T -th stage is evaluated on all classes seen, $\mathcal{C} = \bigcup_{t=1}^T \mathcal{C}_t$, after each incremental task. The disjoint nature of classes across steps t introduces the challenge of *catastrophic forgetting*. As new class sets $\{\mathcal{C}_{t+1}, \mathcal{C}_{t+2}, \dots\}$ arrive, the feature representations and decision boundaries are easily modified, causing the model to forget previously learned classes.

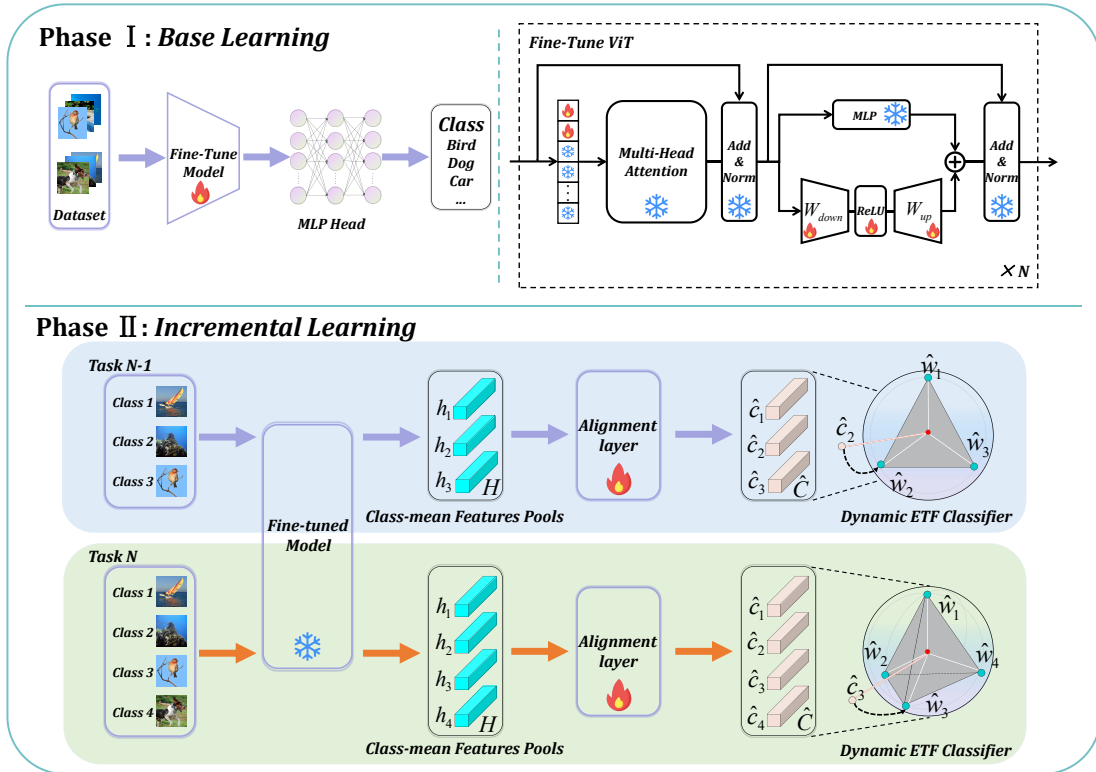


Figure 2. Illustration of NCPTM-CIL. Phase I: Base Learning. We utilize the initial task dataset \mathcal{D}_1 to fine-tune the ViT pre-trained model using the VPT Deep [24] and AdaptFormer [5] methods. Phase II: Incremental Learning. We freeze the fine-tuned ViT pre-trained model to extract the class mean features and store them in Class-Mean Features Pools. Subsequently, these class mean features are aligned and mapped to a Dynamic ETF Classifier through an Alignment layer. It is worth noting that the number of vertices in the Dynamic ETF Classifier is adjusted according to the number of currently learned classes. For example, if the total number of learned classes in Task $N - 1$ is 3, then the number of classifier weight vectors is 3. If the total number of learned classes in Task N is 4, then the number of classifier weight vectors is 4.

3.2. Investigating Catastrophic Forgetting in PTM-based Incremental Learning

This section investigates the catastrophic forgetting phenomenon in pre-trained model-based class incremental learning. Prior studies [37, 62] suggest that deep neural networks progressively enhance linear separability between different classes during training. To validate this hypothesis, we analyze the learning capacity of ViT-B/16-IN1K and ViT-B/16-IN21K pretrained models using the \mathcal{NC}_2 metric (where lower values indicate better linear separability), which measures linear separability through the lens of Simplex Equiangular Tight Frame theory — a mathematical framework that maximizes inter-class variability for optimal classification [38]. We apply the VPT Deep and AdapterFormer methods to fine-tune the pre-trained ViT on the 10-class sampling dataset from VTAB. As shown in Fig. 1a, enhancing inter-class linear separability constitutes the essential learning mechanism in pre-trained model adaptation.

A critical question arises: **Does catastrophic forgetting in PTM-CIL primarily manifest as reduced linear separability for previously learned classes?** To answer this, we monitor \mathcal{NC}_2 trajectories across different PTM-CIL methods on the VTAB dataset during incremental learning

phases. As shown in Fig. 1b, sequential incremental learning phases induce significant \mathcal{NC}_2 elevation (i.e., reduced separability) for previous classes. This empirical evidence supports our conclusion: **Catastrophic forgetting in PTM-CIL essentially stems from the attenuation of inter-class linear separability capacity.**

Motivated by the Simplex ETF framework [75], which minimizes class interference through equiangular tight frame-based feature distribution, we propose employing Dynamic ETF Classifier to guide PTM features towards optimal linear separability states. This approach maintains maximal inter-class separation while ensuring uniform feature space distribution, effectively combating catastrophic forgetting through geometric regularization.

4. Methodology

As discussed earlier, we have confirmed the feasibility of using NC to model PTM-based continual learning. However, in class-incremental learning, the progressive increase in the number of classes across tasks presents a key challenge: *adapting the NC structure to accommodate this growth*. In this section, we introduce our proposed method — NCPTM-CIL — and provide a detailed illustration of the overall training pipeline, the training loss, and the strategy

for dynamically updating the ETF classifier.

4.1. The Overall Pipeline

The proposed NCPTM-CIL operates in two main phases to leverage the strong generalization of pre-trained models for improving class-incremental learning. The overall pipeline is illustrated in Fig. 2.

During the base learning phase, the pre-trained model (ViT, as used in our approach) is fine-tuned on the initial task, adapting it to the target domain while preserving foundational features to support future tasks. Specifically, we employ AdaptFormer [5] and VPT Deep [24] to fine-tune the pre-trained ViT, which inserts trainable low-rank matrices and learnable prompts into the layers of the pre-trained ViT, enabling only these parameters to be updated while keeping the main model weights frozen to swiftly adapting to the new task.

In the incremental learning phase, the fine-tuned model is frozen, and only the added alignment layer is utilized to maintain and evolve the Neural Collapse (NC) structure. This alignment layer takes class means as input to generate the evolving NC structure, ensuring that the principles of neural collapse are preserved during task updates (e.g., transitioning from 3-ETF to 4-ETF, as shown in Fig. 2). Finally, the updated ETF structure can serve as the classifier $\hat{\mathbf{W}}_{\text{ETF}} = [\hat{\mathbf{w}}_1, \dots, \hat{\mathbf{w}}_{K_t}] \in \mathbb{R}^{d \times K_t}$, where $\hat{\mathbf{w}}_k$ is the fixed weight vector for class k in $\hat{\mathbf{W}}_{\text{ETF}}$, and K_t is the total number of classes at current t -th task. During inference, the model computes the maximum similarity between the feature of the instance and K_t classifier vectors to predict the correct category.

$$y_{\text{test}} = \arg \max_{y' \in \{1, \dots, K_t\}} s_{y'},$$

$$s_y = \frac{\mathbf{f}(\mathbf{x}_i)^\top \hat{\mathbf{w}}_k}{\|\mathbf{f}(\mathbf{x}_i)\| \cdot \|\hat{\mathbf{w}}_k\|}. \quad (5)$$

4.2. NC-inspired Function

Dynamic ETF Classifier. In [75]’s method, the Simplex ETF classifier is fixed and non-learnable, requiring prior knowledge of the entire label space across future tasks — a limitation that is impractical for real-world incremental learning scenarios. Dynamic ETF Classifier we propose can increase the number of category prototypes as the number of learned classes grows, thereby better adapting to changes in the real world. Moreover, incorporating the Dynamic ETF Classifier ensures that the class mean features output by the model better align with the \mathcal{NC}_2 characteristics. The formula of the Dynamic ETF Classifier can be constructed as:

$$\hat{\mathbf{W}}_{\text{ETF}} = \sqrt{\frac{K_t}{K_t - 1}} \mathbf{U}_t \left(\mathbf{I}_{K_t} - \frac{1}{K_t} \mathbf{1}_{K_t} \mathbf{1}_{K_t}^\top \right) \quad (6)$$

$\mathbf{U}_t \in \mathbb{R}^{d \times K_t}$ is a dynamically expanded orthogonal matrix satisfying: $\mathbf{U}_t^\top \mathbf{U}_t = \mathbf{I}_{K_t}$.

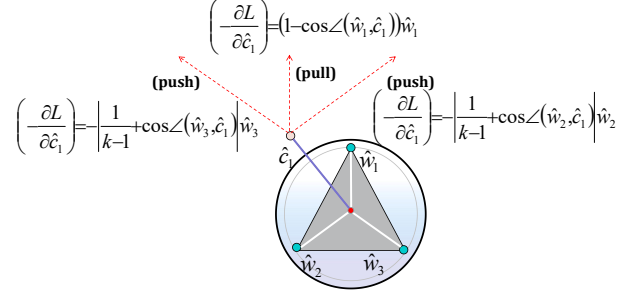


Figure 3. Description of the gradient of PAP Loss with respect to \hat{c}_1 . For PAP Loss, the gradient $(-\frac{\partial \mathcal{L}}{\partial \hat{c}_1})$ pulls \hat{c}_1 towards $\hat{\mathbf{w}}_i$, while the gradients from $(-\frac{\partial \mathcal{L}}{\partial \hat{c}_1})$ and $(-\frac{\partial \mathcal{L}}{\partial \hat{c}_1})$ act as a repulsive force, pushing \hat{c}_1 away from $\hat{\mathbf{w}}_i$ (the red dashed line indicates the direction of the gradient).

Pull And Push Loss. During the incremental learning phase, we design the pull and push (PAP) loss to optimize the parameters of the Alignment layer. This loss function consists of two components: push loss and pull loss. The pull loss drives the class means generated by the PTM to align with their corresponding fixed weight vectors, while the push loss propels class means away from dissimilar vectors. The optimization of PAP loss aims to achieve alignment between the class means extracted by the PTM and the fixed weight vectors in the Dynamic ETF Classifier, thereby maximizing inter-class separability.

$$\mathcal{L}_{\text{PAP}}(\hat{c}_k, \hat{\mathbf{W}}_{\text{ETF}}) = \underbrace{(\hat{\mathbf{w}}_k^\top \hat{c}_k - 1)^2}_{\text{pull}} + \underbrace{\sum_{j \neq k} (\hat{\mathbf{w}}_j^\top \hat{c}_k + \frac{1}{k-1})^2}_{\text{push}}. \quad (7)$$

where \hat{c}_k represents the feature vector derived from the class mean \mathbf{h}^k through the alignment layer. Notably, the gradient of \mathcal{L}_{PAP} with respect to \hat{c}_k is:

$$\left(-\frac{\partial \mathcal{L}_{\text{PAP}}}{\partial \hat{c}_k} \right) = \underbrace{(1 - \cos \angle(\hat{\mathbf{w}}_k, \hat{c}_k)) \hat{\mathbf{w}}_k}_{\text{pull}} - \underbrace{\left(\sum_{j \neq k} \left| \cos \angle(\hat{\mathbf{w}}_j, \hat{c}_k) + \frac{1}{k-1} \right| \hat{\mathbf{w}}_j \right)}_{\text{push}} \quad (8)$$

As shown in Fig. 3, the pull term encourages \hat{c}_k and $\hat{\mathbf{w}}_k$ to align by reducing the angle between their feature vectors. Specifically, when the cosine similarity $\cos \angle(\hat{\mathbf{w}}_k, \hat{c}_k)$ is low, the gradient magnitude becomes larger, and its direction aligns with $\hat{\mathbf{w}}_k$ (as derived in Eq. (8)). This directs \hat{c}_k to be updated towards $\hat{\mathbf{w}}_k$, effectively increasing their similarity. Conversely, the push term penalizes high cosine similarity between \hat{c}_k and negative weight vectors $\hat{\mathbf{w}}_j$ ($j \neq k$).

When $\cos \angle(\hat{\mathbf{w}}_j, \hat{\mathbf{c}}_k)$ is high, the gradient magnitude increases and points away from $\hat{\mathbf{w}}_j$, driving $\hat{\mathbf{c}}_k$ to orthogonalize with irrelevant classifier weights. It can be concluded that global optimality occurs when $\cos \angle(\hat{\mathbf{w}}_k, \hat{\mathbf{c}}_k) = 1$ and $\cos \angle(\hat{\mathbf{w}}_j, \hat{\mathbf{c}}_k) = -\frac{1}{k-1}$, which theoretically demonstrates that the class mean matrix ultimately forms a simplex ETF, satisfying the \mathcal{NC}_2 property.

4.3. ETF Alignment

Considering the feature drift that often occurs in class-incremental learning, using class means to represent the ETF classifier in the current task would lead to significant disruption of the ETF structure. This is where the ALIGNMENT LAYER plays a crucial role. The alignment layer is an MLP block following Hersche [17]. Thanks to the fine-tuning capability of the alignment layer, it helps preserve the orthogonality and separability of previously learned classes during the dynamic update of the ETF. Specifically, in Task t , the class means extracted for each class are stored in the CLASS-MEAN FEATURES POOLS, forming the matrix $\mathbf{H} \in \mathbb{R}^{d \times K_t}$, where K_t is the total number of classes at the current t -th task. The classifier prototypes are initialized as $\hat{\mathbf{W}}_{\text{ETF}} \in \mathbb{R}^{d \times K_t}$. It is important to note that, to prevent the alignment layer parameters from task $t-1$ from negatively impacting the alignment for task t , we initialize a new set of alignment layer parameters for each task to ensure proper alignment during training. The total loss in our framework can be illustrated as:

$$\mathcal{L}_{\text{total}} = \mathcal{L}_{\text{CE}} + \mathcal{L}_{\text{PAP}}. \quad (9)$$

where \mathcal{L}_{CE} denotes the cross-entropy loss.

5. Experiments

In this section, we detail the experimental setup and evaluation metrics, followed by comparisons with state-of-the-art algorithms on five benchmark datasets. Additionally, we conduct an ablation study to assess the robustness of our proposed method and analyze the impact of \mathcal{NC} metrics on model performance. Visualizations are provided in the supplementary material to demonstrate the effectiveness of the model.

5.1. Implementation Details

Dataset: Since pre-trained models often retain extensive knowledge from upstream tasks, following [56, 70], we evaluate performance on CIFAR-100 [27], CUB-200 [48], VTAB [64], and OmniBenchmark [67]. These datasets include standard class-incremental learning benchmarks as well as out-of-distribution datasets with significant domain gaps relative to ImageNet (the dataset used for pre-training). CIFAR-100 contains 100 classes, VTAB includes 50 classes, CUB-200 has 200 classes, and OmniBenchmark

encompasses 300 classes. Additional details are provided in the supplementary material.

Training details: Following [70], we consider two representative models, *i.e.*, ViT-B/16-IN21K and ViT-B/16-IN1K as pre-trained models. The former is pre-trained on ImageNet-21K, and the latter is further fine-tuned on ImageNet-1K. In the base learning phase, we use the SGD optimizer to fine-tune the pre-trained model with a batch size of 48 for 20 epochs of training. The learning rate starts at 0.01, weight decay is set to 0.0005, momentum is 0.9, and cosine annealing scheduling is used. In the incremental learning phase, we use the SGD optimizer to train ALIGNMENT LAYER and employ cosine annealing scheduling. Typically, we perform 40 epochs of training, but in some experiments, this is reduced to fewer epochs if significant overfitting is observed.

Evaluation metrics & Comparison methods: Following [41], we use \mathcal{A}_t to represent the average accuracy across all classes after the t -th stage. We use the accuracy after learning the last task \mathcal{A}_T and the average accuracy across all tasks $\bar{\mathcal{A}} = \frac{1}{T} \sum_{t=1}^T \mathcal{A}_t$ as evaluation metrics. We compare our method with state-of-the-art PTM-based CIL approaches, including L2P [56], DualPrompt [55], CODA-Prompt [44], LAE [11], Aper [70], and EASE [72]. For fairness, all methods are evaluated independently using ViT-B/16 as the pre-trained model.

5.2. Main Results

We compare NCPTM-CIL with other state-of-the-art methods on five standard datasets. Specifically, CIFAR-100, CUB-200, and OmniBenchmark are divided into 10 incremental learning tasks, while VTAB is divided into 5 incremental learning tasks. From the results in Table 1, it can be observed that NCPTM-CIL demonstrates superior performance over all existing methods. To ensure a fair comparison, we also report the performance trend in incremental learning settings across three datasets, as shown in Fig. 4. In these experiments, the base learning phase involves training on half of the total classes, with 5 new classes introduced at each incremental step. The trend plots illustrate that as the number of classes increases, the accuracy of NCPTM-CIL declines only gradually, maintaining a nearly horizontal trajectory compared to other methods. This phenomenon confirms the effectiveness of our method in mitigating catastrophic forgetting. In particular, NCPTM-CIL outperforms the runner-up method by 6.73% on the VTAB dataset, by 1.25% on CIFAR-100, and by 2.5% on OmniBenchmark.

It is well-established that joint learning, which involves integrating old data, represents the upper bound in the continual learning paradigm. We aim to evaluate how closely our approach approximates this theoretical performance limit. Therefore, we conduct a comparative evaluation between our method and joint learning. As shown in Table 2,

Method		Pre-trained	CIFAR-100	CUB-200	VTAB	OmniBenchmark
L2P [56]	CVPR2022	IN21K	87.88	77.45	71.17	74.45
DualPrompt [55]	ECCV2022	IN21K	89.44	84.61	88.37	76.40
CODA-Prompt [44]	CVPR2023	IN21K	91.18	85.11	88.15	73.37
LAE [11]	ICCV2023	IN21K	90.34	83.40	88.92	73.09
Aper [70]	IJCV2024	IN21K	92.25	89.10	90.12	77.30
Ease [72]	CVPR2024	IN21K	92.08	90.12	90.41	75.77
NCPTM-CIL (Ours)		IN21K	93.51	91.22	92.96	80.51

Table 1. Average Top-1 accuracy comparison on four datasets using **ViT-B/16-IN21K** as the backbone. The best performance is highlighted in bold.

Method	Pre-trained	CIFAR-100	CUB-200	VTAB	OmniBenchmark
Joint	IN21K	90.83	86.43	91.58	74.67
NCPTM-CIL (Ours)	IN21K	89.33	85.41	86.94	74.15

Table 2. NCPTM-CIL Last Performance Comparison with the Upper Bound for CIL. “Joint” refers to fine-tuning the pre-trained model using all classes of the dataset, which represents the upper bound in the continual learning paradigm.

our method achieves performance that is nearly on par with joint learning. Specifically, the gap between our method and the incremental learning upper bound is 1.5%, 1.02%, and 0.52% on the CIFAR-100, CUB-200, and OmniBenchmark datasets, respectively.

Dynamic-ETF	Module		CIFAR-100
	Init-Align	PAP Loss	
✓	—	—	92.32
—	✓	—	92.28
—	—	✓	91.92
✓	✓	—	93.25
✓	—	✓	93.07
—	✓	✓	93.21
✓	✓	✓	93.51

Table 3. Ablation study results showing the average Top-1 accuracy after continual learning of all classes on the CIFAR-100 dataset. “Dynamic-ETF” refers to the dynamic ETF classifier, while “Init-Align” denotes the Initial Alignment Layer.

5.3. Ablation Study

To evaluate the contribution of each component in NCPTM-CIL, we conduct an ablation study by removing each module individually. Table 3 shows that removing the Dynamic ETF Classifier results in a noticeable performance drop (from 93.51% to 93.21%), indicating its importance in maintaining the equiangular feature structure aligned with neural collapse. The absence of the Initial Alignment Layer reduces accuracy to 93.07%, highlighting its role in mitigating the negative influence of alignment parameters from previous tasks. This layer ensures that features are optimally aligned for each task, enhancing task-specific adapt-

ability. Excluding PAP Loss leads to a 0.26% drop, suggesting that it enhances feature separability across classes. These results validate the necessity of each component in shaping a robust feature space for incremental learning.

Fine-Tune Method	$\mathcal{N}\mathcal{C}_1$	CIFAR-100
None	0.253	88.436
VPT shallow	0.252	88.518
AdaptFormer	0.132	92.231
Lora	0.107	93.027
VPT Deep	0.101	93.115
AdaptFormer+VPT Deep(NCPTM-CIL)	0.095	93.513

Table 4. Comparison of fine-tuning methods on CIFAR-100. We report the $\mathcal{N}\mathcal{C}_1$ (initial task) and the average top-1 accuracy for each method.

Method	CIFAR-100	$\mathcal{N}\mathcal{C}_2$	$\mathcal{N}\mathcal{C}_3$
NCPTM-CIL	93.51	0.217	0.106
w/o. Dynamic ETF Classifier	93.21	0.259	0.138
w/o. Initial Alignment Layer	93.07	0.471	0.296
w/o. PAP Loss	93.25	0.235	0.125

Table 5. Ablation study results showing the average Top-1 accuracy after continual learning of all classes, along with the average $\mathcal{N}\mathcal{C}_2$ and $\mathcal{N}\mathcal{C}_3$ scores obtained from experiments on the CIFAR-100 dataset.

5.4. Rethinking Incremental Learning

Given the variety of fine-tuning methods for large models, selecting the most suitable method for different datasets can be both time-intensive and computationally costly. Therefore, we aim to identify an efficient selection strategy for

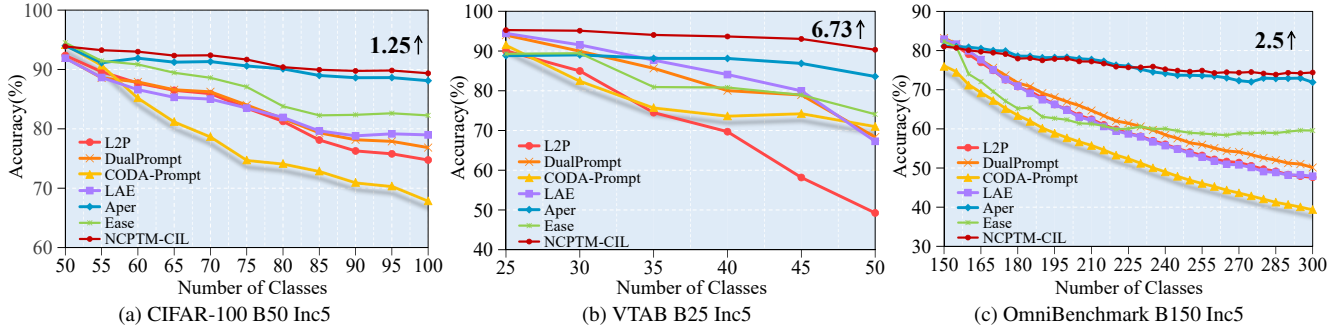


Figure 4. All methods are initialized with **ViT-B/16-IN1K**. We annotate the relative improvement of NCPTM-CIL over the runner-up method with numerical values at the final incremental stage.

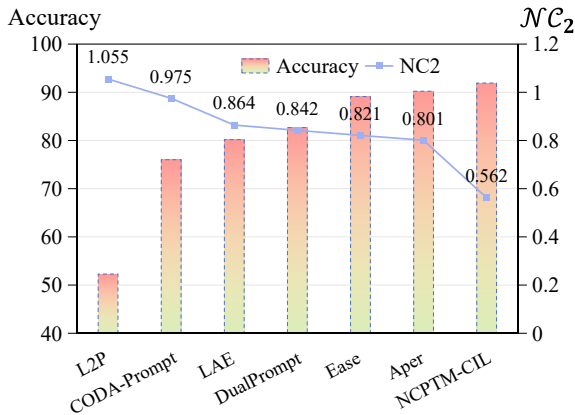


Figure 5. The relationship between the performance of existing PTM-based CIL approaches and their feature’s \mathcal{NC}_2 .

fine-tuning methods from the perspective of NC. Experimentally, we examine the relationship between \mathcal{NC}_1 values in the base learning stage and the final continual learning performance, as shown in Tab. 4. Clearly, when the NC values in phase 1 are better (*i.e.*, lower \mathcal{NC}_1 , indicating better NC), the final continual learning results also improve. This confirms the effectiveness of using NC to model the continual learning distribution and suggests that calculating NC based on first-stage features is sufficient for selecting a suitable fine-tuning method, thereby significantly reducing the time cost of this selection process. Specific details of the fine-tuning methods we used are provided in the supplementary material.

We are also interested in how $\mathcal{NC}_{2\sim 3}$ impacts continual learning, so let us revisit Tab. 5. As shown in Tab. 5, performance declines as key components are removed, and the corresponding \mathcal{NC}_2 and \mathcal{NC}_3 values increase. Note that lower values of \mathcal{NC}_2 and \mathcal{NC}_3 indicate more pronounced NC. Thus, we conclude that the properties of \mathcal{NC}_2 and \mathcal{NC}_3 contribute to a more discriminative continual learning distribution. This effect may be due to the promotion of a self-dual ETF structure formed by the feature means and classifier weights, resulting in a clearer decision boundary. This

aligns with the objective of our PAP loss, further validating the effectiveness of our approach.

To validate if PTM-CIL’s effectiveness stems from the \mathcal{NC}_2 property, we assess PTM-CIL accuracy on VTAB and computed features \mathcal{NC}_2 . All implementations use **ViT-B/16-IN21K** with VTAB split into 10 incremental tasks. As illustrated in Fig. 5, the average task accuracy of PTM-CIL exhibits a significant correlation with \mathcal{NC}_2 . This empirical evidence substantiates that our proposed methodology enhances the linear separability of model-generated features, thereby supporting the hypothesis regarding the critical role of Neural Collapse guidance in facilitating feature evolution during continual learning processes.

6. Conclusion

In this paper, we revisited Class-Incremental Learning (CIL) in the context of pre-trained models (PTMs) and investigated feature evolution through the lens of Neural Collapse (NC) theory. Our analysis revealed that NC, a phenomenon in which class features align equiangularly at the final stage of training, offers a powerful framework for understanding feature evolution across incremental tasks. Building on this insight, we introduced **Neural Collapse-inspired Pre-Trained Model-based CIL (NCPTM-CIL)**, a method designed to maintain a structured and resilient feature space across tasks. Key components of our approach include the **DYNAMIC ETF CLASSIFIER**, **ETF ALIGNMENT**, and **PAP LOSS**, which together maintain a structured and resilient feature space across tasks, thereby effectively mitigating catastrophic forgetting. Extensive experiments validated the effectiveness of our approach, achieving superior performance across multiple benchmarks. These results underscore the efficacy of our NC-inspired design in enabling models to adapt to new classes without forgetting prior ones, marking a significant step forward in leveraging pre-trained models for continual learning.

References

- [1] Tina Behnia, Ganesh Ramachandra Kini, Vala Vakilian, and Christos Thrampoulidis. On the implicit geometry of cross-entropy parameterizations for label-imbalanced data. In *International Conference on Artificial Intelligence and Statistics*, pages 10815–10838. PMLR, 2023. 2
- [2] Pietro Buzzega, Matteo Boschini, Angelo Porrello, Davide Abati, and Simone Calderara. Dark experience for general continual learning: a strong, simple baseline. *Advances in neural information processing systems*, 33:15920–15930, 2020. 2
- [3] Arslan Chaudhry, Puneet K Dokania, Thalaiyasingam Ajanthan, and Philip HS Torr. Riemannian walk for incremental learning: Understanding forgetting and intransigence. In *Proceedings of the European conference on computer vision (ECCV)*, pages 532–547, 2018. 2
- [4] Kai Chen, Jiaqi Wang, Jiangmiao Pang, Yuhang Cao, Yu Xiong, Xiaoxiao Li, Shuyang Sun, Wansen Feng, Ziwei Liu, Jiarui Xu, et al. Mmdetection: Open mmlab detection toolbox and benchmark. *arXiv preprint arXiv:1906.07155*, 2019. 1
- [5] Shoufa Chen, Chongjian Ge, Zhan Tong, Jiangliu Wang, Yibing Song, Jue Wang, and Ping Luo. Adaptformer: Adapting vision transformers for scalable visual recognition. *Advances in Neural Information Processing Systems*, 35:16664–16678, 2022. 4, 5, 1
- [6] MMSegmentation Contributors. MMSegmentation: Openmmlab semantic segmentation toolbox and benchmark. <https://github.com/open-mmlab/mms Segmentation>, 2020. 1
- [7] Alexey Dosovitskiy. An image is worth 16x16 words: Transformers for image recognition at scale. *arXiv preprint arXiv:2010.11929*, 2020. 1
- [8] Arthur Douillard, Matthieu Cord, Charles Ollion, Thomas Robert, and Eduardo Valle. Podnet: Pooled outputs distillation for small-tasks incremental learning. In *Computer vision—ECCV 2020: 16th European conference, Glasgow, UK, August 23–28, 2020, proceedings, part XX 16*, pages 86–102. Springer, 2020. 2
- [9] Cong Fang, Hangfeng He, Qi Long, and Weijie J Su. Exploring deep neural networks via layer-peeled model: Minority collapse in imbalanced training. *Proceedings of the National Academy of Sciences*, 118(43):e2103091118, 2021. 2
- [10] Tomer Galanti, András György, and Marcus Hutter. On the role of neural collapse in transfer learning. *arXiv preprint arXiv:2112.15121*, 2021. 2
- [11] Qiankun Gao, Chen Zhao, Yifan Sun, Teng Xi, Gang Zhang, Bernard Ghanem, and Jian Zhang. A unified continual learning framework with general parameter-efficient tuning. In *Proceedings of the IEEE/CVF International Conference on Computer Vision*, pages 11483–11493, 2023. 6, 7
- [12] Ross Girshick. Fast r-cnn. In *Proceedings of the IEEE International Conference on Computer Vision*, pages 1440–1448, 2015. 1
- [13] Florian Graf, Christoph Hofer, Marc Niethammer, and Roland Kwitt. Dissecting supervised contrastive learning. In *International Conference on Machine Learning*, pages 3821–3830. PMLR, 2021. 2
- [14] XY Han, Vardan Papyan, and David L Donoho. Neural collapse under mse loss: Proximity to and dynamics on the central path. *arXiv preprint arXiv:2106.02073*, 2021. 2
- [15] Kaiming He, Xiangyu Zhang, Shaoqing Ren, and Jian Sun. Deep residual learning for image recognition. In *Proceedings of the IEEE/CVF conference on Computer Vision and Pattern Recognition*, pages 770–778, 2016. 1
- [16] Kaiming He, Xiangyu Zhang, Shaoqing Ren, and Jian Sun. Identity mappings in deep residual networks. In *Computer Vision—ECCV 2016: 14th European Conference*, 2016. 1
- [17] Michael Hersche, Geethan Karunaratne, Giovanni Cherubini, Luca Benini, Abu Sebastian, and Abbas Rahimi. Constrained few-shot class-incremental learning. In *Proceedings of the IEEE/CVF conference on computer vision and pattern recognition*, pages 9057–9067, 2022. 6
- [18] Geoffrey Hinton. Distilling the knowledge in a neural network. *arXiv preprint arXiv:1503.02531*, 2015. 2
- [19] Saihui Hou, Xinyu Pan, Chen Change Loy, Zilei Wang, and Dahua Lin. Learning a unified classifier incrementally via rebalancing. In *Proceedings of the IEEE/CVF conference on computer vision and pattern recognition*, pages 831–839, 2019. 2
- [20] Edward J Hu, Yelong Shen, Phillip Wallis, Zeyuan Allen-Zhu, Yuanzhi Li, Shean Wang, Lu Wang, and Weizhu Chen. Lora: Low-rank adaptation of large language models. *arXiv preprint arXiv:2106.09685*, 2021. 1
- [21] Jie Hu, Li Shen, and Gang Sun. Squeeze-and-excitation networks. In *Proceedings of the IEEE Conference on Computer Vision and Pattern Recognition*, pages 7132–7141, 2018. 1
- [22] Chenxi Huang, Liang Xie, Yibo Yang, Wenxiao Wang, Binbin Lin, and Deng Cai. Neural collapse inspired federated learning with non-iid data. *arXiv preprint arXiv:2303.16066*, 2023. 2
- [23] Wenlong Ji, Yiping Lu, Yiliang Zhang, Zhun Deng, and Weijie J Su. An unconstrained layer-peeled perspective on neural collapse. *arXiv preprint arXiv:2110.02796*, 2021. 2
- [24] Menglin Jia, Luming Tang, Bor-Chun Chen, Claire Cardie, Serge Belongie, Bharath Hariharan, and Ser-Nam Lim. Visual prompt tuning. In *European Conference on Computer Vision*, pages 709–727. Springer, 2022. 4, 5, 1
- [25] Minsoo Kang, Jaeyoo Park, and Bohyung Han. Class-incremental learning by knowledge distillation with adaptive feature consolidation. In *Proceedings of the IEEE/CVF conference on computer vision and pattern recognition*, pages 16071–16080, 2022. 2
- [26] James Kirkpatrick, Razvan Pascanu, Neil Rabinowitz, Joel Veness, Guillaume Desjardins, Andrei A Rusu, Kieran Milan, John Quan, Tiago Ramalho, Agnieszka Grabska-Barwinska, et al. Overcoming catastrophic forgetting in neural networks. *Proceedings of the national academy of sciences*, 114(13):3521–3526, 2017. 2
- [27] Alex Krizhevsky, Geoffrey Hinton, et al. Learning multiple layers of features from tiny images. 2009. 6
- [28] Sang-Woo Lee, Jin-Hwa Kim, Jaehyun Jun, Jung-Woo Ha, and Byoung-Tak Zhang. Overcoming catastrophic forget-

- ting by incremental moment matching. *Advances in neural information processing systems*, 30, 2017. 2
- [29] Brian Lester, Rami Al-Rfou, and Noah Constant. The power of scale for parameter-efficient prompt tuning. *arXiv preprint arXiv:2104.08691*, 2021. 1
- [30] Xiao Li, Sheng Liu, Jinxin Zhou, Xinyu Lu, Carlos Fernandez-Granda, Zihui Zhu, and Qing Qu. Principled and efficient transfer learning of deep models via neural collapse. *arXiv preprint arXiv:2212.12206*, 2022. 2
- [31] Zhizhong Li and Derek Hoiem. Learning without forgetting. *IEEE transactions on pattern analysis and machine intelligence*, 40(12):2935–2947, 2017. 2
- [32] Tsung-Yi Lin, Piotr Dollár, Ross Girshick, Kaiming He, Bharath Hariharan, and Serge Belongie. Feature pyramid networks for object detection. In *Proceedings of the IEEE conference on computer vision and pattern recognition*, pages 2117–2125, 2017. 1
- [33] Yu Liu, Xiaopeng Hong, Xiaoyu Tao, Songlin Dong, Jingang Shi, and Yihong Gong. Model behavior preserving for class-incremental learning. *IEEE Transactions on Neural Networks and Learning Systems*, 34(10):7529–7540, 2022. 2
- [34] Jianfeng Lu and Stefan Steinerberger. Neural collapse under cross-entropy loss. *Applied and Computational Harmonic Analysis*, 59:224–241, 2022. 2
- [35] Mark D McDonnell, Dong Gong, Ehsan Abbasnejad, and Anton van den Hengel. Premonition: Using generative models to preempt future data changes in continual learning. *arXiv preprint arXiv:2403.07356*, 2024. 1, 2
- [36] Dustin G Mixon, Hans Parshall, and Jianzong Pi. Neural collapse with unconstrained features. *Sampling Theory, Signal Processing, and Data Analysis*, 20(2):11, 2022. 2
- [37] Vardan Papyan. Traces of class/cross-class structure pervade deep learning spectra. *Journal of Machine Learning Research*, 21(252):1–64, 2020. 4
- [38] Vardan Papyan, XY Han, and David L Donoho. Prevalence of neural collapse during the terminal phase of deep learning training. *Proceedings of the National Academy of Sciences*, 117(40):24652–24663, 2020. 2, 3, 4
- [39] Tomaso Poggio and Qianli Liao. Explicit regularization and implicit bias in deep network classifiers trained with the square loss. *arXiv preprint arXiv:2101.00072*, 2020. 2
- [40] Ameya Prabhu, Philip HS Torr, and Puneet K Dokania. Gdumb: A simple approach that questions our progress in continual learning. In *Computer Vision—ECCV 2020: 16th European Conference, Glasgow, UK, August 23–28, 2020, Proceedings, Part II 16*, pages 524–540. Springer, 2020. 2
- [41] Sylvestre-Alvise Rebuffi, Alexander Kolesnikov, Georg Sperl, and Christoph H Lampert. icarl: Incremental classifier and representation learning. In *Proceedings of the IEEE conference on Computer Vision and Pattern Recognition*, pages 2001–2010, 2017. 2, 6
- [42] Andrei A Rusu, Neil C Rabinowitz, Guillaume Desjardins, Hubert Soyer, James Kirkpatrick, Koray Kavukcuoglu, Razvan Pascanu, and Raia Hadsell. Progressive neural networks. *arXiv preprint arXiv:1606.04671*, 2016. 2
- [43] Joan Serra, Didac Suris, Marius Miron, and Alexandros Karatzoglou. Overcoming catastrophic forgetting with hard attention to the task. In *International conference on machine learning*, pages 4548–4557. PMLR, 2018. 2
- [44] James Seale Smith, Leonid Karlinsky, Vyshnavi Gutta, Paola Cascante-Bonilla, Donghyun Kim, Assaf Arbelle, Rameswar Panda, Rogerio Feris, and Zsolt Kira. Coda-prompt: Continual decomposed attention-based prompting for rehearsal-free continual learning. In *Proceedings of the IEEE/CVF Conference on Computer Vision and Pattern Recognition*, pages 11909–11919, 2023. 1, 2, 6, 7
- [45] Christos Thrampoulidis, Ganesh Ramachandra Kini, Vala Vakilian, and Tina Behnia. Imbalance trouble: Revisiting neural-collapse geometry. *Advances in Neural Information Processing Systems*, 35:27225–27238, 2022. 2
- [46] Tom Tirer and Joan Bruna. Extended unconstrained features model for exploring deep neural collapse. In *International Conference on Machine Learning*, pages 21478–21505. PMLR, 2022. 2
- [47] Laurens Van der Maaten and Geoffrey Hinton. Visualizing data using t-sne. *JMLR*, 9(11), 2008. 1
- [48] Catherine Wah, Steve Branson, Peter Welinder, Pietro Perona, and Serge Belongie. The caltech-ucsd birds-200-2011 dataset. 2011. 6
- [49] Liyuan Wang, Bo Lei, Qian Li, Hang Su, Jun Zhu, and Yi Zhong. Triple-memory networks: A brain-inspired method for continual learning. *IEEE Transactions on Neural Networks and Learning Systems*, 33(5):1925–1934, 2021. 2
- [50] Liyuan Wang, Kuo Yang, Chongxuan Li, Lanqing Hong, Zhenguo Li, and Jun Zhu. Ordisco: Effective and efficient usage of incremental unlabeled data for semi-supervised continual learning. In *Proceedings of the IEEE/CVF Conference on Computer Vision and Pattern Recognition*, pages 5383–5392, 2021. 2
- [51] Liyuan Wang, Xingxing Zhang, Qian Li, Jun Zhu, and Yi Zhong. Coscl: Cooperation of small continual learners is stronger than a big one. In *European Conference on Computer Vision*, pages 254–271. Springer, 2022. 2
- [52] Liyuan Wang, Xingxing Zhang, Kuo Yang, Longhui Yu, Chongxuan Li, Lanqing Hong, Shifeng Zhang, Zhenguo Li, Yi Zhong, and Jun Zhu. Memory replay with data compression for continual learning. *arXiv preprint arXiv:2202.06592*, 2022. 2
- [53] Liyuan Wang, Jingyi Xie, Xingxing Zhang, Mingyi Huang, Hang Su, and Jun Zhu. Hierarchical decomposition of prompt-based continual learning: Rethinking obscured sub-optimality. *Advances in Neural Information Processing Systems*, 36, 2024. 2
- [54] Siwei Wang and Stephanie E Palmer. Towards understanding neural collapse in supervised contrastive learning with the information bottleneck method. *arXiv preprint arXiv:2305.11957*, 2023. 2
- [55] Zifeng Wang, Zizhao Zhang, Sayna Ebrahimi, Ruoxi Sun, Han Zhang, Chen-Yu Lee, Xiaoqi Ren, Guolong Su, Vincent Perot, Jennifer Dy, et al. Dualprompt: Complementary prompting for rehearsal-free continual learning. In *European Conference on Computer Vision*, pages 631–648. Springer, 2022. 1, 2, 6, 7

- [56] Zifeng Wang, Zizhao Zhang, Chen-Yu Lee, Han Zhang, Ruoxi Sun, Xiaoqi Ren, Guolong Su, Vincent Perot, Jennifer Dy, and Tomas Pfister. Learning to prompt for continual learning. In *Proceedings of the IEEE/CVF conference on computer vision and pattern recognition*, pages 139–149, 2022. 1, 2, 6, 7
- [57] Stephan Wojtowytsch et al. On the emergence of simplex symmetry in the final and penultimate layers of neural network classifiers. *arXiv preprint arXiv:2012.05420*, 2020. 2
- [58] Yue Wu, Yinpeng Chen, Lijuan Wang, Yuancheng Ye, Zicheng Liu, Yandong Guo, and Yun Fu. Large scale incremental learning. In *Proceedings of the IEEE/CVF conference on computer vision and pattern recognition*, pages 374–382, 2019. 2
- [59] Liang Xie, Yibo Yang, Deng Cai, and Xiaofei He. Neural collapse inspired attraction–repulsion-balanced loss for imbalanced learning. *Neurocomputing*, 527:60–70, 2023. 2
- [60] Binbin Yang, Xinchu Deng, Han Shi, Changlin Li, Gengwei Zhang, Hang Xu, Shen Zhao, Liang Lin, and Xiaodan Liang. Continual object detection via prototypical task correlation guided gating mechanism. In *Proceedings of the IEEE/CVF conference on computer vision and pattern recognition*, pages 9255–9264, 2022. 2
- [61] Yibo Yang, Shixiang Chen, Xiangtai Li, Liang Xie, Zhouchen Lin, and Dacheng Tao. Inducing neural collapse in imbalanced learning: Do we really need a learnable classifier at the end of deep neural network? *Advances in neural information processing systems*, 35:37991–38002, 2022. 2
- [62] John Zarka, Florentin Guth, and Stéphane Mallat. Separation and concentration in deep networks. *arXiv preprint arXiv:2012.10424*, 2020. 4
- [63] Friedemann Zenke, Ben Poole, and Surya Ganguli. Continual learning through synaptic intelligence. In *International conference on machine learning*, pages 3987–3995. PMLR, 2017. 2
- [64] Xiaohua Zhai, Joan Puigcerver, Alexander Kolesnikov, Pierre Ruysen, Carlos Riquelme, Mario Lucic, Josip Djolonga, Andre Susano Pinto, Maxim Neumann, Alexey Dosovitskiy, et al. A large-scale study of representation learning with the visual task adaptation benchmark. *arXiv preprint arXiv:1910.04867*, 2019. 6
- [65] Gengwei Zhang, Liyuan Wang, Guoliang Kang, Ling Chen, and Yunchao Wei. Slca: Slow learner with classifier alignment for continual learning on a pre-trained model. In *Proceedings of the IEEE/CVF International Conference on Computer Vision*, pages 19148–19158, 2023. 1
- [66] Junting Zhang, Jie Zhang, Shalini Ghosh, Dawei Li, Serafettin Tasci, Larry Heck, Heming Zhang, and C-C Jay Kuo. Class-incremental learning via deep model consolidation. In *Proceedings of the IEEE/CVF winter conference on applications of computer vision*, pages 1131–1140, 2020. 2
- [67] Yuanhan Zhang, Zhenfei Yin, Jing Shao, and Ziwei Liu. Benchmarking omni-vision representation through the lens of visual realms. In *European Conference on Computer Vision*, pages 594–611. Springer, 2022. 6
- [68] Hengshuang Zhao, Jianping Shi, Xiaojuan Qi, Xiaogang Wang, and Jiaya Jia. Pyramid scene parsing network. In *Proceedings of the IEEE Conference on Computer Vision and Pattern Recognition*, pages 2881–2890, 2017. 1
- [69] Zhisheng Zhong, Jiequan Cui, Yibo Yang, Xiaoyang Wu, Xiaojuan Qi, Xiangyu Zhang, and Jiaya Jia. Understanding imbalanced semantic segmentation through neural collapse. In *Proceedings of the IEEE/CVF conference on computer vision and pattern recognition*, pages 19550–19560, 2023. 1, 2
- [70] Da-Wei Zhou, Zi-Wen Cai, Han-Jia Ye, De-Chuan Zhan, and Ziwei Liu. Revisiting class-incremental learning with pre-trained models: Generalizability and adaptivity are all you need. *International Journal of Computer Vision*, pages 1–21, 2024. 1, 2, 6, 7
- [71] Da-Wei Zhou, Hai-Long Sun, Jingyi Ning, Han-Jia Ye, and De-Chuan Zhan. Continual learning with pre-trained models: A survey. *arXiv preprint arXiv:2401.16386*, 2024. 2
- [72] Da-Wei Zhou, Hai-Long Sun, Han-Jia Ye, and De-Chuan Zhan. Expandable subspace ensemble for pre-trained model-based class-incremental learning. In *Proceedings of the IEEE/CVF Conference on Computer Vision and Pattern Recognition*, pages 23554–23564, 2024. 1, 2, 6, 7
- [73] Jinxin Zhou, Xiao Li, Tianyu Ding, Chong You, Qing Qu, and Zhihui Zhu. On the optimization landscape of neural collapse under mse loss: Global optimality with unconstrained features. In *International Conference on Machine Learning*, pages 27179–27202. PMLR, 2022. 2
- [74] Yitao Zhu, Zhenrong Shen, Zihao Zhao, Sheng Wang, Xin Wang, Xiangyu Zhao, Dinggang Shen, and Qian Wang. Melo: Low-rank adaptation is better than fine-tuning for medical image diagnosis. In *2024 IEEE International Symposium on Biomedical Imaging (ISBI)*, pages 1–5. IEEE, 2024. 1
- [75] Zhihui Zhu, Tianyu Ding, Jinxin Zhou, Xiao Li, Chong You, Jeremias Sulam, and Qing Qu. A geometric analysis of neural collapse with unconstrained features. *Advances in Neural Information Processing Systems*, 34:29820–29834, 2021. 2, 4, 5

Enhancing Pre-Trained Model-Based Class-Incremental Learning through Neural Collapse

Supplementary Material

1. Experimental Settings

In this section, we provide an overview of the datasets employed in our study:

CIFAR-100: This dataset comprises 60,000 images spanning 100 classes, with 50,000 images designated for training and 10,000 for testing. Each class includes 100 images.

CUB-200: Widely used for fine-grained visual classification tasks, this dataset contains 11,788 images across 200 bird species. The training set has 9,430 images, while the test set includes 2,358 images.

OmniBenchmark: This dataset contains 89,697 training images and 5,985 testing images across 300 diverse classes. Due to the large domain gaps between classes, OmniBenchmark poses a greater challenge for incremental learning compared to other datasets.

VTAB: This dataset supports cross-domain incremental learning across five domains. It consists of 1,796 training images and 8,619 testing images covering 50 classes.

2. Fine-tuning methods

We experimented with four fine-tuning methods for the ViT-B/16 pretrained model: LoRA [74], AdaptFormer [5], VPT Deep, and VPT Shallow [24].

LoRA: The core idea of LoRA [20] is to freeze the weights of the pretrained model and decompose its weight matrices into low-rank matrices, thus reducing the number of trainable parameters and improving fine-tuning efficiency. Following the approach in [74], we inject LoRA weights into the query projection matrix W_Q and value projection matrix W_V of each self-attention layer in ViT. The formulation can be expressed as:

$$y = W_0x + BAx \quad (1)$$

where $x \in \mathbb{R}^{k \times d}$ and $x \in \mathbb{R}^{k \times d}$ represent the input and output features, respectively. $W_0 \in \mathbb{R}^{d \times d}$ denotes the pretrained weights for either W_Q or W_V , while $B \in \mathbb{R}^{d \times r}$ and $A \in \mathbb{R}^{r \times d}$ are the trainable low-rank matrices. We set the rank of the low-rank matrices to $r = 8$ significantly smaller than the model dimension $d = 768$. By using LoRA, we greatly reduce the number of trainable parameters, enhancing training efficiency.

AdaptFormer: AdaptFormer focuses on fine-tuning the MLP layers of ViT. It introduces two projection matrices: W^{down} for dimensionality reduction, and W^{up} to project the reduced feature back to the original dimension. Given

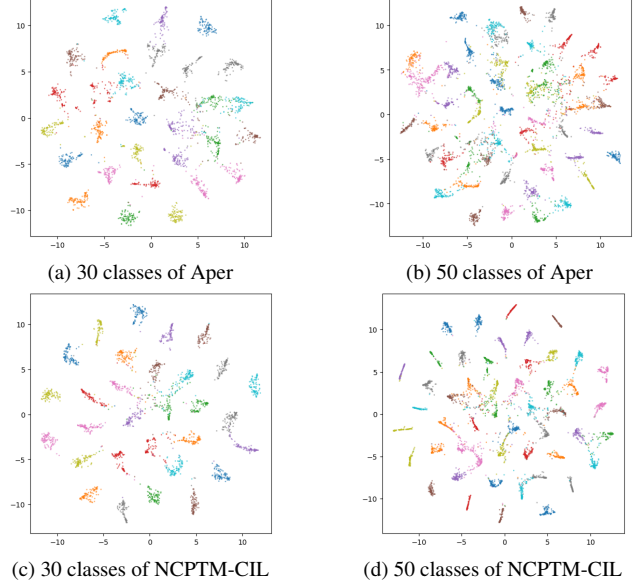


Figure 6. **Top:** t-SNE [47] visualization of the features of the Aper algorithm on the CIFAR-100 test dataset with 30 and 50 classes. **Bottom:** t-SNE visualization of the features of NCPTM-CIL on the CIFAR-100 test dataset with 30 and 50 classes.

an input $x \in \mathbb{R}^{k \times d}$, the AdaptFormer output is computed as:

$$y = \text{MLP}(x) + \text{ReLU}(W^{\text{down}}x)W^{\text{up}} \quad (2)$$

where $W^{\text{down}} \in \mathbb{R}^{d \times r}$ and $W^{\text{up}} \in \mathbb{R}^{r \times d}$. We set the rank $r = 64$, much smaller than the model dimension $d = 768$. During fine-tuning, MLP parameters are frozen, and only the two projection matrices are trained, reducing the computational cost.

VPT: VPT adds learnable parameters $\mathbf{P} \in \mathbb{R}^{p \times d}$ to the image encoding features $x \in \mathbb{R}^{k \times d}$, forming the final expanded feature:

$$x' = [x; p] \quad (3)$$

where $x' \in \mathbb{R}^{(k+p) \times d}$ is the input to the subsequent layers of ViT. VPT has two variants: VPT Shallow, which attaches the trainable parameters \mathbf{P} only at the first layer of the pretrained model, and VPT Deep, which attaches \mathbf{P} at every layer of the pretrained model.

3. Visualizations

In Fig. 6, we present a t-SNE comparison of feature distributions between the Aper and NCPTM-CIL on the CIFAR-100 test dataset under different incremental tasks, specifically for 30 and 50 classes. Fig. 6a and Fig. 6b illustrate

the feature distributions of the Aper for 30 and 50 classes, respectively. As new classes are introduced, Aper’s feature distributions become more entangled, with less separation between classes. In contrast, Fig. 6c and Fig. 6d show the feature distributions of our proposed NCPTM-CIL method under the same settings. Benefiting from guidance by the Neural Collapse geometry, NCPTM-CIL achieves better class separation, maintaining a more balanced and distinct feature distribution even as the number of classes increases.

This visualization further confirms the effectiveness of our approach. By aligning the feature space with the Neural Collapse structure, NCPTM-CIL dynamically adjusts the feature distribution to maintain inter-class separation and consistency, thereby enhancing adaptability to new tasks and stability to previous ones in the continual learning process. In contrast to traditional methods, this demonstrates that leveraging pre-trained models in combination with NC geometry effectively captures feature evolution in class-incremental learning.